

## Space-Time Domain Decomposition for Mixed Formulations of Diffusion Equations

Thi Thao Phuong Hoang, Jérôme Jaffré, Caroline Japhet, Michel Kern, Jean Roberts

► **To cite this version:**

Thi Thao Phuong Hoang, Jérôme Jaffré, Caroline Japhet, Michel Kern, Jean Roberts. Space-Time Domain Decomposition for Mixed Formulations of Diffusion Equations. 21st International Conference on Domain Decomposition Methods, Jun 2012, Rennes, France. Springer, 2013. <hal-00923353>

**HAL Id: hal-00923353**

**<https://hal.inria.fr/hal-00923353>**

Submitted on 2 Jan 2014

**HAL** is a multi-disciplinary open access archive for the deposit and dissemination of scientific research documents, whether they are published or not. The documents may come from teaching and research institutions in France or abroad, or from public or private research centers.

L'archive ouverte pluridisciplinaire **HAL**, est destinée au dépôt et à la diffusion de documents scientifiques de niveau recherche, publiés ou non, émanant des établissements d'enseignement et de recherche français ou étrangers, des laboratoires publics ou privés.

# Space-Time Domain Decomposition for Mixed Formulations of Diffusion Equations <sup>\*</sup>

Thi-Thao-Phuong Hoang<sup>1</sup>, Jérôme Jaffré<sup>1</sup>, Caroline Japhet<sup>1,2</sup>, Michel Kern<sup>1</sup> and Jean Roberts<sup>1</sup>

**Key words:** mixed finite elements, time-dependent Steklov-Poincaré operator, optimized Schwarz waveform relaxation.

## 1 Introduction

Flow and transport problems in porous media are well-known for their high computational cost. In the far field simulation of an underground nuclear waste disposal site, one has to work with extremely different length and time scales, and highly variable coefficients while satisfying strict accuracy requirements. One strategy for tackling these difficulties is to apply a non-overlapping domain decomposition method which allows local adaptation in both space and time and makes possible the use of parallel algorithms. The substructuring method with a Steklov Poincaré operator, which is widely used by engineers for steady problems with strong heterogeneities, is a promising option. The optimized Schwarz waveform relaxation (OSWR) method, which has been developed over the last decade for finite element and finite volume methods, is another potential choice.

The objective of this paper is twofold. Firstly, we propose the time-dependent Steklov Poincaré operator and introduce the Neumann-Neumann preconditioner [2] as well as the weight matrices [13] to improve the convergence speed and handle the heterogeneities. Secondly, we extend the OSWR approach [8] to the case of mixed finite elements [3] with their local mass-conservation property. Numerical experiments in 2D are presented to illustrate the performance of the two methods for a simplified ANDRA<sup>\*</sup> test case.

For an open, bounded subset  $\Omega$  of  $\mathbb{R}^d$  ( $d = 2, 3$ ) with Lipschitz boundary  $\partial\Omega$  and some fixed time  $T > 0$ , we consider the following time-dependent diffusion problem

$$\omega \partial_t c + \nabla \cdot (-\mathbf{D} \nabla c) = f \text{ in } \Omega \times (0, T), \quad (1)$$

$$c = 0 \text{ on } \partial\Omega \times (0, T), \quad (2)$$

$$c(0, \cdot) = c_0 \text{ in } \Omega, \quad (3)$$

where  $c$  is the concentration of a contaminant,  $\omega$  the porosity and  $\mathbf{D}$  a symmetric, positive definite diffusion tensor.

We now rewrite (1) in an equivalent mixed form by introducing the vector field  $\mathbf{r} := -\mathbf{D} \nabla c$ . This yields

---

<sup>1</sup> INRIA, Rocquencourt, France, e-mail: {Phuong.Hoang\_Thi\_Thao}{Jerome.Jaffre}{Michel.Kern}{Jean.Roberts}@inria.fr <sup>2</sup> Université Paris 13, LAGA, Villetaneuse, France, e-mail: japhet@math.univ-paris13.fr

<sup>\*</sup> This work was supported by ANDRA, the French Agency for Nuclear Waste Management.

$$\begin{aligned}\omega \partial_t c + \nabla \cdot \mathbf{r} &= f \text{ in } \Omega \times (0, T), \\ \mathbf{D}^{-1} \mathbf{r} + \nabla c &= 0 \text{ in } \Omega \times (0, T),\end{aligned}\quad (4)$$

along with boundary and initial conditions (2) - (3). Henceforth, unless otherwise specified, we implicitly assume boundary condition (2) on  $\partial\Omega$ .

**Theorem 1.** (Well-posedness and Regularity)

Suppose that the diffusion tensor  $\mathbf{D}$  is in  $W^{1,\infty}(\Omega)^{d^2}$ . If  $f \in L^2(0, T; L^2(\Omega))$  and  $c_0 \in H_0^1(\Omega)$ , then problem (4) has a unique weak solution  $(c, \mathbf{r})$  such that

$$c \in H^1(0, T; L^2(\Omega)) \text{ and } \mathbf{r} \in L^2(0, T; H(\operatorname{div}, \Omega)) \cap L^\infty(0, T; L^2(\Omega)^d).$$

Moreover, if  $f \in H^1(0, T; L^2(\Omega))$  and  $c_0 \in H^2(\Omega) \cap H_0^1(\Omega)$  then

$$c \in W^{1,\infty}(0, T; L^2(\Omega)) \text{ and } \mathbf{r} \in L^\infty(0, T; H(\operatorname{div}, \Omega)) \cap H^1(0, T; L^2(\Omega)^d).$$

The proof is based on energy estimates and Galerkin's method (see [12, 9]).

## 2 Two space-time domain decomposition methods

Our work relies on the decomposition of  $\Omega$  into non-overlapping subdomains. For simplicity, we describe the methods in case of two non-overlapping subdomains  $\Omega_1$  and  $\Omega_2$  with  $\Gamma = \partial\Omega_1 \cap \partial\Omega_2 \cap \Omega$  (the results can be extended to the case of many subdomains as we shall see in the numerical experiments).

Let  $\{c_i, \mathbf{r}_i\}$  be the restriction to  $\Omega_i$ ,  $i = 1, 2$ , of  $\{c, \mathbf{r}\}$ , the solution to (4). Problem (4) can be reformulated in the equivalent multi-domain form by solving the same problem (globally in space and time) in each subdomain:

$$\begin{aligned}\omega_i \partial_t c_i + \nabla \cdot \mathbf{r}_i &= f \text{ in } \Omega_i \times (0, T) \\ \mathbf{D}_i^{-1} \mathbf{r}_i + \nabla c_i &= 0 \text{ in } \Omega_i \times (0, T) \quad \text{for } i = 1, 2, \\ c_i(0) &= c_0 \text{ in } \Omega_i\end{aligned}\quad (5)$$

along with the physical transmission conditions on the space-time interface

$$\begin{aligned}c_1 &= c_2 \\ \mathbf{r}_1 \cdot \mathbf{n}_1 + \mathbf{r}_2 \cdot \mathbf{n}_2 &= 0 \quad \text{on } \Gamma \times (0, T).\end{aligned}\quad (6)$$

where  $\mathbf{n}_i$  is the outward unit normal vector on  $\partial\Omega_i$ .

### 2.1 Method 1: Time-dependent Steklov-Poincaré operator approach

This method is the continuous counterpart of the Schur complement method, but extended to the time-dependent problem.

For  $f$  and  $c_0$  as before and  $\lambda \in L^2(0, T; H^{\frac{1}{2}}(\Gamma))$ , we define the extension operators

$$\mathcal{D}_i : (\lambda, f, c_0) \mapsto (c_i(\lambda, f, c_0), \mathbf{r}_i(\lambda, f, c_0)),$$

where  $(c_i(\lambda, f, c_0), \mathbf{r}_i(\lambda, f, c_0))$ ,  $i = 1, 2$ , is the solution to the problem

$$\begin{aligned}\omega_i \partial_t c_i + \nabla \cdot \mathbf{r}_i &= f \text{ in } \Omega_i \times (0, T), \\ \mathbf{D}_i^{-1} \mathbf{r}_i + \nabla c_i &= 0 \text{ in } \Omega_i \times (0, T), \\ c_i &= \lambda \text{ on } \Gamma \times (0, T), \\ c_i(0) &= c_0 \text{ in } \Omega_i.\end{aligned}\quad (7)$$

Comparing with (5), (6),  $(c_i(\lambda, f, c_0), \mathbf{r}_i(\lambda, f, c_0))$  satisfies (5) - (6) if and only if

$$\mathbf{r}_1(\lambda, f, c_0) \cdot \mathbf{n}_1 + \mathbf{r}_2(\lambda, f, c_0) \cdot \mathbf{n}_2 = 0 \quad \text{on } \Gamma \times (0, T),$$

or equivalently,

$$\mathcal{F}_1 \mathcal{D}_1(\lambda, f, c_0) + \mathcal{F}_2 \mathcal{D}_2(\lambda, f, c_0) = 0 \quad \text{on } \Gamma \times (0, T), \quad (8)$$

where  $\mathcal{F}_i(c_i, \mathbf{r}_i) := \mathbf{r}_i \cdot \mathbf{n}_i|_{\Gamma}$ ,  $i = 1, 2$ , is the normal trace operator.

As the operators  $\mathcal{F}_i$  and  $\mathcal{D}_i$  are affine in  $\lambda$ , (8) can be rewritten as

$$\mathcal{S}\lambda = \chi \quad \text{on } \Gamma \times (0, T), \quad (9)$$

where  $\mathcal{S}$  is the linear time-dependent Steklov-Poincaré operator, defined by

$$\mathcal{S} = \mathcal{S}_1 + \mathcal{S}_2, \quad \mathcal{S}_i \lambda := -\mathcal{F}_i \mathcal{D}_i(\lambda, 0, 0) \quad (\text{Dirichlet-to-Neumann operator}).$$

And the right-hand side is

$$\chi = \mathcal{F}_1 \mathcal{D}_1(0, f, c_0) + \mathcal{F}_2 \mathcal{D}_2(0, f, c_0).$$

**Remark.**

(i) Subdomain problem (7) is wellposed (this is an easy extension of Theorem 1).

(ii) We solve problem (9) iteratively using a Krylov subspace method such as GMRES.

(ii) The operator  $\mathcal{S}$  is non-symmetric. In particular, by writing the variational formulations of the subdomain problems, we deduce for  $\lambda, \eta \in L^2(0, T; H^{\frac{1}{2}}(\Gamma))$  that

$$\langle \mathcal{S}\lambda, \eta \rangle = \sum_{i=1}^2 \left( \int_0^T \int_{\Omega_i} \mathbf{D}^{-1} \tilde{\mathbf{r}}_i(\eta) \cdot \tilde{\mathbf{r}}_i(\lambda) + \int_0^T \int_{\Omega_i} \omega_i \frac{\partial \tilde{c}_i(\lambda)}{\partial t} \tilde{c}_i(\eta) \right),$$

where  $(\tilde{c}_i(\lambda), \tilde{\mathbf{r}}_i(\lambda)) := \mathcal{D}_i(\lambda, 0, 0)$  for  $i = 1, 2$ . Thus, the well-posedness of (9) is still an open question (see a related work by F. Kwok [11]).

## 2.2 Method 2: Optimized Schwarz waveform relaxation approach

We consider the second domain decomposition approach, the Optimized Schwarz Waveform Relaxation (OSWR) method, where we replace the physical transmission conditions (6) by the equivalent Robin conditions on the space-time interface

$$\begin{aligned} -\mathbf{r}_1 \cdot \mathbf{n}_1 + p_1 c_1 &= -\mathbf{r}_2 \cdot \mathbf{n}_1 + p_1 c_2 \\ -\mathbf{r}_2 \cdot \mathbf{n}_2 + p_2 c_2 &= -\mathbf{r}_1 \cdot \mathbf{n}_2 + p_2 c_1 \end{aligned} \quad \text{on } \Gamma \times (0, T), \quad (10)$$

where  $p_1$  and  $p_2$  are positive parameters that can be optimized to significantly improve the convergence rate of the method (see [1, 4, 5] and the references therein).

The OSWR method may be written as follows: at the  $k^{\text{th}}$  iteration, we solve in each subdomain the problem

$$\begin{aligned}
\partial_t c_i^k + \nabla \cdot \mathbf{r}_i^k &= f && \text{in } \Omega_i \times (0, T), \\
\mathbf{D}_i^{-1} \mathbf{r}_i^k + \nabla c_i^k &= 0 && \text{in } \Omega_i \times (0, T), \\
-\mathbf{r}_i^k \cdot \mathbf{n}_i + p_i c_i^k &= -\mathbf{r}_j^{k-1} \cdot \mathbf{n}_i + p_i c_j^{k-1} && \text{on } \Gamma \times (0, T), \quad j = (3-i), \\
c_i(0, \cdot) &= c_0 && \text{in } \Omega_i.
\end{aligned} \tag{11}$$

**Remark.**

(i) For the first iteration, the transmission conditions are replaced by

$$-\mathbf{r}_i^1 \cdot \mathbf{n}_i + p_i c_i^1 = g_i, \quad \text{on } \Gamma \times (0, T)$$

for  $g_i, i = 1, 2$ , an initial guess on the space-time interface.

(ii) The well-posedness of subdomain problem (11) is an extension of Theorem 1 (see [9]) making use of the space  $\mathcal{H}(\text{div}, \Omega_i)$  defined by

$$\mathcal{H}(\text{div}, \Omega_i) = \{ \mathbf{v} \in H(\text{div}, \Omega_i) \text{ such that } \mathbf{v} \cdot \mathbf{n}_i \in L^2(\Gamma) \}.$$

**Theorem 2.** (Convergence of the OSWR method in mixed form)

Suppose that  $\mathbf{D}$  is in  $W^{1,\infty}(\Omega)^{d^2}$ . Let  $f \in H^1(0, T; L^2(\Omega))$  and  $c_0 \in H^2(\Omega) \cap H_0^1(\Omega)$ . If the algorithm (11) is initialized by  $(g_i)$  given in  $H^1(0, T; L^2(\Gamma))$ , then it defines a unique sequence of iterates

$(c_i^k, \mathbf{r}_i^k) \in W^{1,\infty}(0, T; L^2(\Omega_i)) \times L^\infty(0, T; \mathcal{H}(\text{div}, \Omega_i)) \cap H^1(0, T; L^2(\Omega_i)^d)$ ,  $i = 1, 2$ , that converges to the weak solution  $(c, \mathbf{r})$  of problem (4).

**Remark.** Theorem 2 can be extended to the case of many subdomains (see [9]).

As in subsection 2.1, we now derive an interface problem. However, here we use two interface unknowns: let  $\zeta_i \in H^1(0, T; L^2(\Gamma))$ ,  $i = 1, 2$ . We define the following extension operators:

$$\mathcal{B}_i : (\zeta_i, f, c_0) \mapsto (c_i(\zeta_i, f, c_0), \mathbf{r}_i(\zeta_i, f, c_0)), \tag{12}$$

where  $(c_i(\zeta_i, f, c_0), \mathbf{r}_i(\zeta_i, f, c_0))$ ,  $i = 1, 2$ , is the solution to the problem

$$\begin{aligned}
\omega_i \partial_t c_i + \nabla \cdot \mathbf{r}_i &= f && \text{in } \Omega_i \times (0, T), \\
\mathbf{D}_i^{-1} \mathbf{r}_i + \nabla c_i &= 0 && \text{in } \Omega_i \times (0, T), \\
-\mathbf{r}_i \cdot \mathbf{n}_i + p_i c_i &= \zeta_i && \text{on } \Gamma \times (0, T), \\
c_i(0) &= c_0 && \text{in } \Omega_i.
\end{aligned} \tag{13}$$

The interface operators are denoted by  $\mathcal{B}_i$ ,  $i = 1, 2$ , and are defined by

$$\mathcal{B}_i(c_j, \mathbf{r}_j) = (-\mathbf{r}_j \cdot \mathbf{n}_i + p_i c_j) |_\Gamma, \quad j = (3-i). \tag{14}$$

Thus, transmission conditions (10) lead to the interface problem

$$\begin{aligned}
\zeta_1 &= \mathcal{B}_1 \mathcal{B}_2(\zeta_2, f, c_0) \\
\zeta_2 &= \mathcal{B}_2 \mathcal{B}_1(\zeta_1, f, c_0)
\end{aligned} \quad \text{on } \Gamma \times (0, T), \tag{15}$$

or equivalently,

$$\begin{pmatrix} I & -\mathcal{B}_1\mathcal{R}_2(\cdot, 0, 0) \\ -\mathcal{B}_2\mathcal{R}_1(\cdot, 0, 0) & I \end{pmatrix} \begin{pmatrix} \zeta_1 \\ \zeta_2 \end{pmatrix} = \begin{pmatrix} \mathcal{B}_1\mathcal{R}_2(0, f, c_0) \\ \mathcal{B}_2\mathcal{R}_1(0, f, c_0) \end{pmatrix} \text{ on } \Gamma \times (0, T).$$

We solve this system iteratively using Jacobi iteration (this is the OSWR method (11)) or using GMRES.

### 3 Discontinuous Galerkin time stepping with different subdomain time grids

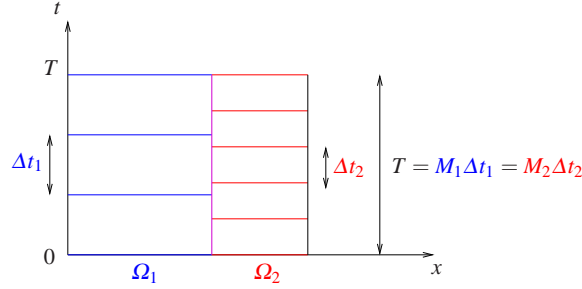


Fig. 1: Non-conforming time grids in the subdomains.

As the two methods described in the previous section are global in time, we can use different time steps in different subdomains according to their physical properties. We consider two possibly different uniform partitions  $\mathcal{T}_1$  and  $\mathcal{T}_2$  of the time interval  $(0, T)$  into sub-intervals of lengths  $\Delta t_1$  and  $\Delta t_2$  respectively. We denote by  $J_m^i$  the interval  $(t_{m-1}^i, t_m^i]$ ,  $m = 1, \dots, M_i$ , for  $i = 1, 2$ . In particular, we are interested in the non-conforming case where  $\Delta t_1 \neq \Delta t_2$  as depicted in Fig. 1. For the time discretization, we use the discontinuous Galerkin method [10, 8]. In this paper, we consider the lowest order scheme, which is a modified backward Euler method. We denote by  $P_0(\mathcal{T}_i, W)$  the space of piecewise constant functions in time on grid  $\mathcal{T}_i$  with values in  $W$  where  $W = H^{\frac{1}{2}}(\Gamma)$  for Method 1 and  $W = L^2(\Gamma)$  for Method 2:

$$P_0(\mathcal{T}_i, W) = \{ \phi : (0, T) \rightarrow W, \phi \text{ is constant in time on } J_m^i, \forall m = 1, \dots, M_i \}.$$

In order to exchange data on the space-time interface between different time grids, we define the following  $L^2$  projection  $\Pi_{ji}$  from  $P_0(\mathcal{T}_i, W)$  onto  $P_0(\mathcal{T}_j, W)$ : for  $\phi \in P_0(\mathcal{T}_i, W)$ ,  $\Pi_{ji}\phi|_{J_m^j}$  is the average value of  $\phi$  on  $J_m^i$ , for  $m = 1, \dots, M_j$ . We use a simple algorithm [6] for effectively performing this projection. With these tools, we are now able to weakly enforce the transmission conditions over the time intervals.

**For Method 1.** We take  $\lambda$  piecewise constant in time (on grid  $\mathcal{T}_1$ , or  $\mathcal{T}_2$  or on yet another grid). Let, for instance,  $\lambda \in P_0(\mathcal{T}_1, H^{\frac{1}{2}}(\Gamma))$ . Thus, we have

$$c_1 = \Pi_{11}(\lambda) = \text{Id}(\lambda) \text{ and } c_2 = \Pi_{21}(\lambda), \quad \text{on } \Gamma \times (0, T).$$

The flux is then conserved over each time interval  $J_m^1$  by letting

$$\int_{J_m^1} (\Pi_{11}(\mathbf{r}_1(\Pi_{11}(\lambda))) \cdot \mathbf{n}_1 + \Pi_{12}(\mathbf{r}_2(\Pi_{21}(\lambda))) \cdot \mathbf{n}_2) dt = 0, \quad \text{for } m = 1, \dots, M_1.$$

**For Method 2.** As we have two Lagrange multipliers on the space-time interface, we take  $\zeta_i \in P_0(\mathcal{T}_i, L^2(\Gamma))$  for  $i = 1, 2$  and enforce the conservation of the jumps of the two Robin terms over the time intervals [8] by letting

$$\int_{J_m^i} (\zeta_i - \Pi_{ij}(-\mathbf{r}_j(\zeta_j) \cdot \mathbf{n}_i + p_i c_j(\zeta_j))) dt = 0,$$

for  $m = 1, \dots, M_i$ , and for  $i = 1, 2, j = (3 - i)$ .

## 4 Numerical Experiments

We consider 2D problems with  $\mathbf{D} = d\mathbf{I}$  isotropic and constant in each subdomain, where  $\mathbf{I}$  is the identity matrix. We then denote by  $d_i := d|_{\Omega_i}$ .

**For Method 1: Using a Neumann-Neumann Preconditioner.** In the elliptic case with strong heterogeneity, the convergence of an iterative method for the Schur complement problem enhanced with a Neumann-Neumann preconditioner and weight matrices is independent of the jump in the coefficients [13]. Thus, we extend the idea to our method for parabolic problem. In particular, we rewrite the interface problem (9) as

$$(\delta_1 \mathcal{S}_1^{-1} + \delta_2 \mathcal{S}_2^{-1})(\mathcal{S}_1 + \mathcal{S}_2)\lambda = \hat{\chi} \quad \text{on } \Gamma \times (0, T),$$

where  $\delta_i = [d_i / (d_1 + d_2)]^2$  and  $\mathcal{S}_i^{-1}$ , the Neumann-to-Dirichlet operator, is the inverse of  $\mathcal{S}_i$  for  $i = 1, 2$ . This formula can be generalized to the case of many subdomains.

**For Method 2: Using two optimization techniques.** To calculate the optimized Robin parameters for discontinuous coefficients, the first approach is to optimize the convergence factor based on the two-half space Fourier analysis [4], we call this approach Opt. 1. In our application to nuclear waste problems where the geometry consists of small objects embedded in a large space, we use an adapted optimization proposed in [7], called Opt. 2, which takes into account the size of the subdomains.

We consider a test case designed by ANDRA for the pure diffusion equation. The

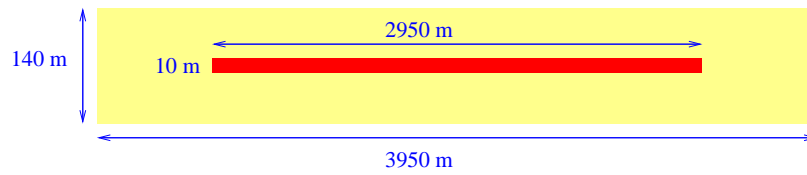


Fig. 2: Geometry of the domain.

geometry of the physical domain is depicted in Fig. 2. The porosity is  $\omega = 0.2$  in the repository (in red) and  $\omega = 0.05$  in the clay layer (in yellow). The diffusion coefficient is  $d = 2 \times 10^{-9} \text{ m}^2 \text{ s}^{-1}$  in the repository and  $d = 5 \times 10^{-12} \text{ m}^2 \text{ s}^{-1}$  in the clay layer. The source term is

$$f = \begin{cases} 10^{-5} \text{ mol/s} & \text{if } t \leq 10^5 \text{ years,} \\ 0 & \text{if } t > 10^5 \text{ years,} \end{cases}$$

in the repository, and  $f = 0$  in the clay layer.

For the spatial discretization, we use a non-uniform rectangular mesh with a finer discretization in the repository (a uniform mesh with 600 points in the x direction and 30 points in the y direction) and a coarser discretization in the clay layer (the mesh size progressively increases with distance to the repository by a factor of 1.05). We then apply mixed finite elements with the lowest order Raviart-Thomas space on rectangles. For the time discretization, we use non-matching time grids with  $\Delta t = 2000$  years in the repository and  $\Delta t = 10000$  years in the clay layer. Finally, we decompose the domain into 9 rectangular subdomains ( $3 \times 3$  with the repository represented by one subdomain).

To analyze and compare the convergence results of different algorithms, we solve a

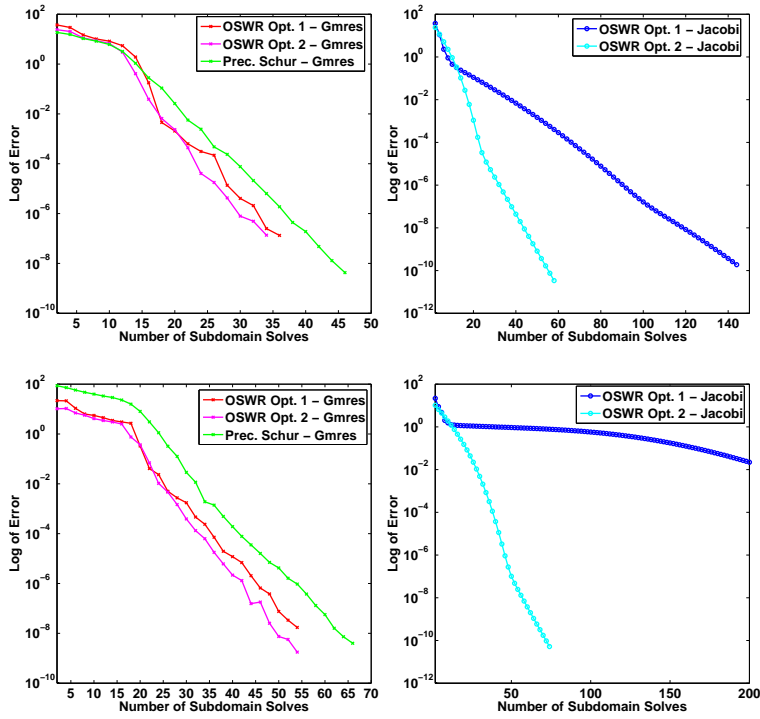


Fig. 3: Convergence curves for different algorithms and time intervals: with GMRES (on the left) and with Jacobi (on the right), for short time  $T = 200,000$  years (on top) and for long time  $T = 1,000,000$  years (on below).

problem with the right hand side  $f \equiv 0$ . We start with random initial guesses on the space-time interfaces and check the convergence to zero in  $L^2(0, T; L^2(\Omega))$ -norms of the concentration and vector field, with tolerance  $10^{-6}$  on the residual. We re-



mark that one iteration of Method 1 with the preconditioner costs twice as much as one iteration of Method 2 (in terms of number of subdomain solves). Thus we plot the error versus the number of subdomain solves (instead of versus the number of iterations). In Fig. 3, we compare the errors for different algorithms (GMRES on the left and Jacobi iteration on the right) and over different time intervals (shorter interval on top and longer interval on bottom). The same time steps,  $\Delta t_i$ , are used for the shorter and longer time intervals. We observe that with GMRES, both Method 1 (with Neumann-Neumann preconditioner) and Method 2 (with either Opt. 1 or Opt. 2) work well and their performance is comparable. The convergence becomes slower when the time interval increases, which is reasonable and expected. On the other hand, with Jacobi iteration, we see that the performance of Opt. 1 (classical) is far behind Opt. 2 (adapted), especially for the long time case.

## References

1. Bennequin, D., Gander, M.J., Halpern, L.: A homographic best approximation problem with application to optimized Schwarz waveform relaxation. *Math. Comput.* **78**, 185–223 (2009)
2. DeRoeck, Y.H., Tallec, P.L.: Analysis and test of a local domain decomposition preconditioner. In: R. Glowinski, Y. Kuznetsov, G. Meurant, J. Périaux, O. Widlund (eds.) *Proceedings of the 4th International Symposium on Domain Decomposition Methods for Partial Differential Equations*. SIAM, Philadelphia, PA (1991)
3. Douglas, J., Leme, P.P., Roberts, J., Wang, J.: A parallel iterative procedure applicable to the approximate solution of second order partial differential equations by mixed finite element methods. *Numer. Math.* **65**, 95–108 (1993)
4. Gander, M.J., Halpern, L., Kern, M.: A Schwarz waveform relaxation method for advection-diffusion-reaction problems with discontinuous coefficients and non-matching grids. In: O. Widlund, D.E. Keyes (eds.) *Decomposition Methods in Science and Engineering XVI*, Heidelberg, pp. 916–920. Springer (2007)
5. Gander, M.J., Halpern, L., Nataf, F.: Optimized Schwarz waveform relaxation method for the one dimensional wave equation. *SIAM J. Numer. Anal.* **41**(5) (2003)
6. Gander, M.J., Japhet, C., Maday, Y., Nataf, F.: A new cement to glue non-conforming grids with Robin interface conditions: The finite element case. In: R. Kornhuber, R.H.W. Hoppe, J. Périaux, O. Pironneau, O.B. Widlund, J. Xu (eds.) *Proceedings of the 5th International Conference on Domain Decomposition Methods*, vol. 40, pp. 259–266. Springer LNCSE (2005)
7. Halpern, L., Japhet, C., Omnes, P.: Nonconforming in time domain decomposition method for porous media applications. In: J.C.F. Pereira, A. Sequeira (eds.) *Proceedings of the 5th European Conference on Computational Fluid Dynamics ECCOMAS CFD 2010*. Lisbon, Portugal (2010)
8. Halpern, L., Japhet, C., Szeftel, J.: Discontinuous Galerkin and nonconforming in time optimized Schwarz waveform relaxation. In: Y. Huang, R. Kornhuber, O. Widlund, J. Xu (eds.) *Domain Decomposition Methods in Science and Engineering XIX*, pp. 133–140 (2011)
9. Hoang, T.T.P., Jaffré, J., Japhet, C., Kern, M., Roberts, J.E.: Domain decomposition methods for time-dependent diffusion problems in mixed formulations. Research report, N° 8271, HAL: inria-00803796 (<http://hal.inria.fr/hal-00803796/>) (2013)
10. Johnson, C., Eriksson, K., Thomée, V.: Time discretization of parabolic problems by discontinuous Galerkin method. *RAIRO Modél. Math. Anal. Numér.* **19** (1995)
11. Kwok, F.: Neumann-Neumann waveform relaxation for the time-dependent heat equation. In: *This proceedings*
12. Li, J., Arbogast, T., Huang, Y.: Mixed methods using standard conforming finite elements. *Comput. Methods Appl. Mech. Engrg.* **198**, 680–692 (2009)
13. Mandel, J., Brezina, M.: Balancing domain decomposition for problems with large jumps in coefficients. *Math. Comput.* **65**, 1387–1401 (1996)